Analysis of Alignment Tolerant Hybrid Optoelectronic Receivers for High Density Interconnection Substrates

Michael Vrazel, Jae J. Chang, Martin Brooke, Nan M. Jokerst, Youngjoong Joo, Lawrence Carastro, Georgianna Dagnall, April Brown
School of Electrical and Computer Engineering
Georgia Institute of Technology
Atlanta, GA 30332
E-mail: mvrazel@ee.gatech.edu

Abstract

High frequency signal distribution in HDI/HDW substrates can be achieved using optical interconnections. To realize effective milli- and micro-haul interconnections on these substrates, the hybrid integration of independently optimized interface circuits and optoelectronic detectors is critical. Further, to realize effective cost goals, designing the optoelectronic interface for alignment tolerance is a key goal. This paper describes the design, fabrication, and test of hybrid integrated optoelectronic interface circuits designed for alignment tolerance and for integration onto an HDI/HDW substrate.

Introduction

As the signal speeds and wiring complexity of high density interconnection (HDI) and high density wiring (HDW) substrates rises, interconnection limitations such as latency become difficult electrical issues. The introduction of optical signal distribution, in particular, for low latency clock signals, is a viable solution to the electrical interconnection issues if the optoelectronics can be integrated into the HDI/HDW system. The hybrid integration of independently optimized thin film optoelectronic components onto Si CMOS VLSI circuitry, which can then be bump bonded onto an HDI/HDW substrate, enables the implementation of optoelectronic integrated circuits (OEICs) in milli- and micro-haul communication links. Historically, optoelectronic link interfaces have been optimized for long haul, low loss applications, where the few optical interfaces necessary could be relatively high cost. To shift the optical interconnection paradigm to lower cost, shorter haul systems, use of appropriate devices coupled with alignnment tolerant optical packaging designs can significantly impact the cost of the link. In addition, microsystems demand a high level of integration and miniaturization, which can both be achieved through hybrid integration. In this paper, we report upon highly alignment tolerant optoelectronic devices in thin film form bonded directly to foundry Si CMOS interface circuits which have been designed for bump bonding onto an HDI/HDW substrate to create an optical interconnection link to the substrate. The HDI/HDW OE interface substrate has been designed with integral decoupling capacitors, and the improved signal recovery with these integral passives is also discussed herein.

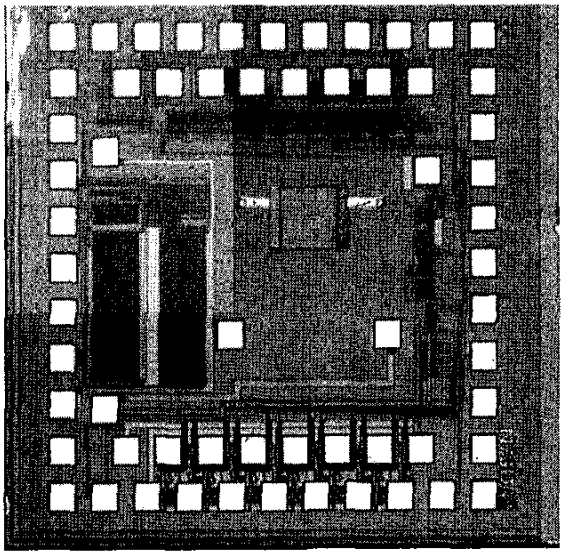

Figure 1: Si CMOS VLSI differential receiver circuit integrated with InGaAs/InP I-MSM photodetector

To achieve alignment tolerant optoelectronic integrated receivers, MSM photodetectors are attractive since they are high speed, large area photodetectors with moderate responsivity and a significantly larger capacitance per unit area than PIN detectors at high speed. However, to achieve highly alignment tolerant operation, the responsivity of the MSMs must be increased. In this paper, we report on the integration of an inverted (I-) MSM which has the metallic fingers on the bottom of the device, rather than on the top. Such an integration scheme is possible with thin film MSM detectors, which are approximately 1 micron thick. We have demonstrated that these I-MSMs have responsivities which are comparable to PIN detectors, are larger than PINs, are high speed, and can be integrated with Si CMOS foundry circuits, as shown in the photomicrograph in Figure 1 [1]. The circuit in Figure 1 consists of a thin film InP/InGaAs (λ=1.3μm) I-MSM metal/metal bonded to a Si CMOS differential receiver circuit (for operation in a noisy digital environment), which has been tested with an open eye diagram at 414 Mbps.

To design an alignment tolerant receiver, modeling which includes the circuit and optoelectronic devices and the optical coupling is critical. Using a receiver circuit design such as that shown in Figure 1, the input capacitance to the receiver is set (e.g. to 0.1-0.5 pF), which in turns dictates detector characteristics. This paper will compare the size and

absorbing thickness of PIN, MSM, and I-MSM photodetectors dictated by this capacitance. Using Gaussian beam (for lasers) and Lambertian (for LEDs) optical inputs, the output current as a function of position for each of these detectors will be evaluated, resulting in an alignment tolerance estimate for the link based upon the minimum input current that the receiver can tolerate. Thus, the alignment tolerance of the fully hybrid integrated system can be estimated and optimized to minimize packaging cost.

Alignment Tolerance Modeling

Multiple factors must be considered to accurately predict the alignment tolerance of a particular receiver. Detector area and responsivity play a significant role in determining alignment tolerance. A detector with a large area or a high responsivity will exhibit a greater degree of alignment tolerance than a detector that is either smaller or has a lower responsivity, respectively. Another significant aspect used to predict alignment tolerance is the type of beam used as an optical source. Lambertian sources, such as LEDs, will provide a large transverse alignment tolerance for an optical link, while a much more directional source, such as a laser Gaussian beam, will typically provide better longitudinal alignment tolerance.

The first step in predicting the alignment tolerance of a receiver is to estimate the fraction of incident optical power that is absorbed by the detector. For Gaussian beams, this step is relatively straightforward. By computing the overlap integral of the beam intensity with detector area, the fraction of the total power of the beam that is incident on the detector is determined. Using the absorption coefficient of the detector material, the thickness of the detecting region, and the responsivity of the detector, a first-order approximation for the photocurrent can be calculated. As the longitudinal and transverse alignment of the optical source (laser or fiber) is shifted, the resulting changes in photocurrent can be examined to determine the alignment tolerance of the receiver.

For Lambertian sources, the overlap integral of beam intensity and detector area can become very complicated and computationally involved. For this reason, the Fast Fourier Transform (FFT) method described by Wang, et. al. [2] is used to simplify the computations. In this method, the overlap integral (which is essentially a convolution integral) is calculated by multiplying the Fourier transforms of the beam intensity, detector area, and emitter area and taking the inverse Fourier transform of the result in order to obtain the power incident on the detector. Once again, using the material parameters of the detector, a first-order approximation for the photocurrent can be obtained and studied for different longitudinal and transversal misalignments.

In this model, for both types of beams, the assumption is made that the sources emit a total power of 1 mW. The beams were also attenuated as they propagated through the optical fiber so that the total power of the beam upon exiting the fiber was assumed to be 10 μW. The differential receiver circuit shown in Figure 1 requires a minimum input detector current of 2.3 μA, and the investigated photodetectors were modeled using these specifications as well as the receiver input capacitance.

The three types of photodetectors investigated in this paper are conventional PINs, conventional MSMs, and I-MSMs. PINs have traditionally been used in applications requiring high photodetector responsivity, whereas conventional MSMs are favored for systems which demand a large degree of alignment tolerance. MSMs have a low capacitance per unit area compared to PINs, so for the same value of capacitance, an MSM typically has a surface area up to three times larger than a PIN. However, MSMs characteristically have low responsivities due to the shadowing induced by the interdigitated surface metal electrodes. Inverted (I-) MSMs are an alternative photodetector that eliminates this tradeoff between high responsivity and low capacitance per unit area. By inverting a conventional MSM (i.e., putting the fingers on the bottom of the device) finger shadowing is eliminated, and by removing the substrate, substrate optical losses are eliminated. I-MSMs have shown only minimal reductions in speed compared to conventional MSMs. The receiver circuit (shown in Figure 1) is designed for operation with a photodetector that has 0.1 – 0.5 pF capacitance.

The photodetectors modeled in this paper are a 50x50 μm^2 InGaAs PIN photodetector as described in [3], a 200x200 μm^2 InGaAs MSM with 2 μm fingers and 4 μm spacings, an I-MSM of similar material and dimensions, a 250x250 μm^2 InGaAs MSM with 2 μm fingers and 5 μm spacings, and an I-MSM of similar material and dimensions. The calculated capacitance of the 200x200 μm^2 MSMs (conventional and inverted) is 0.35 pF, while the 250x250 μm^2 MSMs have a calculated capacitance of 0.43 pF. The 250x250 μm^2 I-MSMs have been fabricated and integrated onto pads as well as hybrid integrated onto foundry Si CMOS receiver circuits. The measured responsivity for these devices is 0.50 A/W. For the purpose of these simulations the responsivity of the 200x200 μm^2 I-MSMs will be assumed to be 0.50 A/W as well. The PINs used for this comparison have a capacitance of 0.35 pF and a responsivity of 0.70 A/W [3].

Based on shadowing loss due to the metal fingers, the responsivity of a 200x200 μm^2 conventional MSM with the same feature sizes as the corresponding I-MSM described

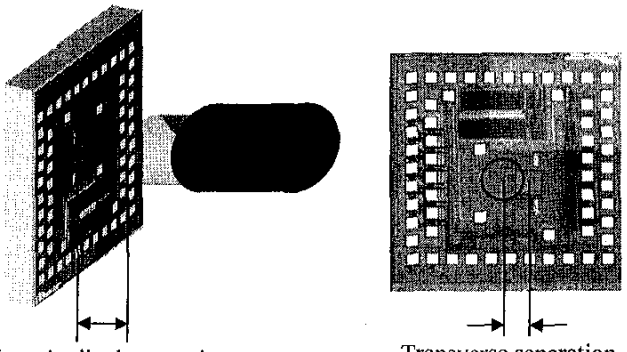

Figure 2: Illustration of longitudinal and transverse alignment tolerance

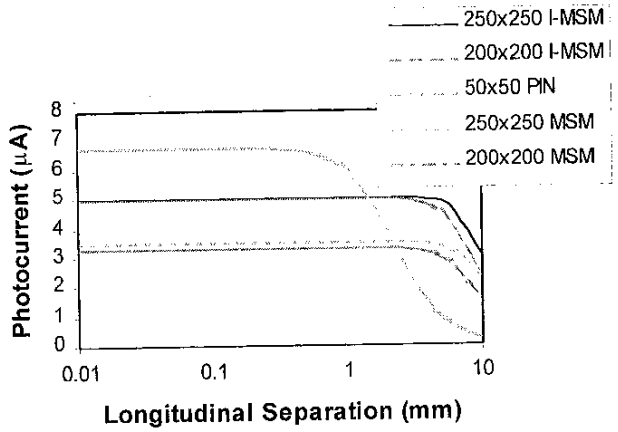

Figure 3: Photocurrent from I-MSMs, MSMs, and PIN as a function of longitudinal separation for Gaussian beam input.

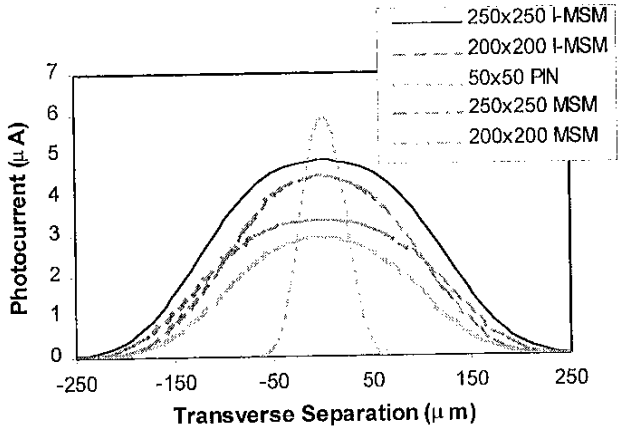

Figure 4: Photocurrent from I-MSMs, MSMs, and PIN as a function of transverse separation for Gaussian beam input.

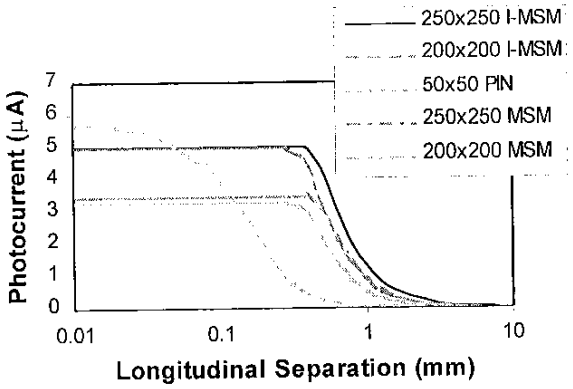

Figure 5: Photocurrent from I-MSMs, MSMs, and PIN as a function of transverse separation for Lambertian beam input.

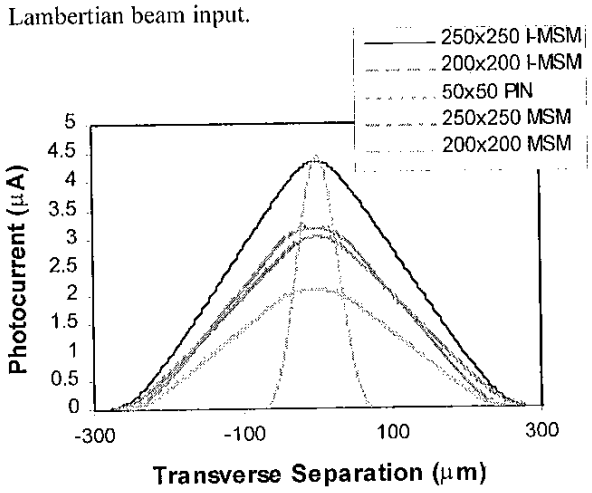

Figure 6: Photocurrent from I-MSMs, MSMs, and PIN as a function of transverse separation for Lambertian beam input.

above is estimated to be 0.33 A/W, and the responsivity of a 250x250 μm^2 conventional MSM with the same features as the I-MSM of similar size has a calculated value of 0.35 A/W.

The capacitances of all of the devices listed above are suited for integration into the receiver circuit shown in Figure 1. The MSMs and I-MSMs have larger detecting areas due to their low capacitance per unit area and therefore will operate with a much better degree of alignment tolerance compared to the PIN. This becomes clearly evident when investigating the maximum misalignments between fiber and detector for which the 2.3 μA of photocurrent necessary for receiver operation can still be generated by the photodetector. The MSMs and I-MSMs can tolerate much greater fiber to detector misalignments than the PINs.

Two types of alignment tolerance are investigated in this paper: longitudinal alignment tolerance and transverse alignment tolerance. The alignment tolerance of an optical link is determined by the ability of the link to tolerate separations and misalignments between the linked optical components. Figure 2 illustrates longitudinal and lateral separation. Longitudinal separation in a fiber to detector link refers to the distance between the edge of the fiber and the surface of the detector whereas transverse separation is defined as the distance between the center of the fiber as projected onto the plane of the circuit and the center of the photodetector. The I-MSMs, MSMs, and PINs were investigated for both of these types of alignment tolerance.

The modeling data presented in this paper includes both plastic and glass multimode optical fibers. The step index glass fiber used for this study had a 62.5 μm core diameter and a numerical aperture of 0.275. Plastic step index optical fibers with core diameters of 240 μm and NA = 0.51 were also investigated. Plastic optical fiber is of particular interest for low-cost OE interfaces such as in home fiber optic backbones and EMI insensitive links for automotive applications. For Gaussian beam modeling, the modeled fibers were step index, with the power primarily confined to the LP_{01} mode. For short lengths of fiber, relatively little mode coupling will occur.

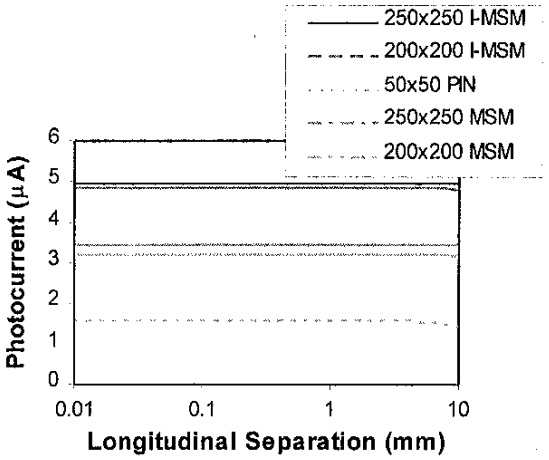

Figure 7: Photocurrent from I-MSMs, MSMs, and PINs as a function of longitudinal separation for Gaussian beam input.

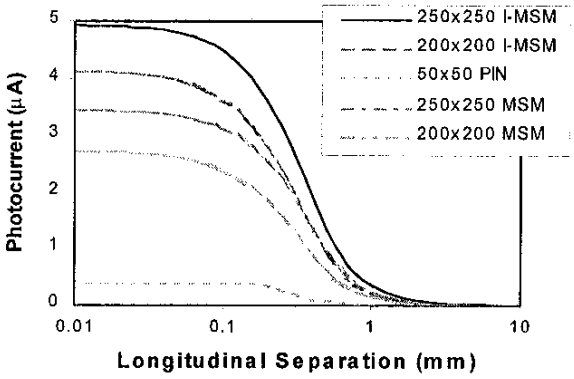

Figure 9: Photocurrent from I-MSMs, MSMs, and PINs as a function of longitudinal separation for Lambertian beam input.

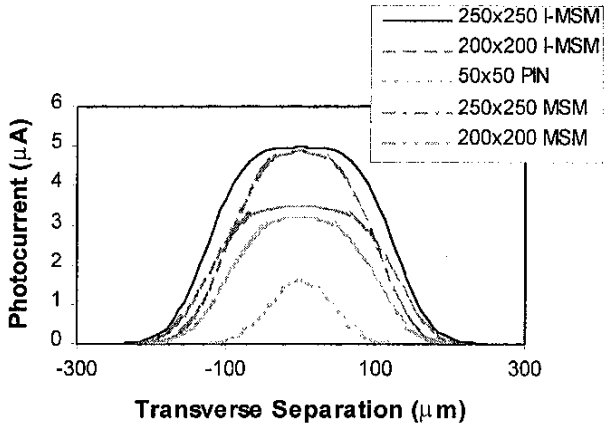

Figure 8: Photocurrent from I-MSMs, MSMs, and PINs as a function of transverse separation for Gaussian beam input.

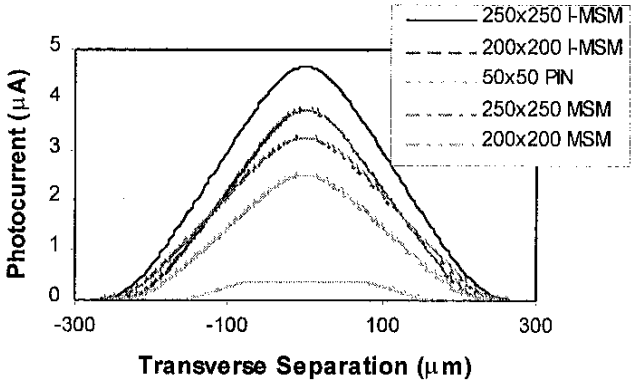

Figure 10: Photocurrent from I-MSMs, MSMs, and PINs as a function of longitudinal separation for Lambertian beam input.

Figures 3 and 4 compare the alignment tolerance of the PIN, MSMs, and I-MSMs for Gaussian beams coupled from the glass fiber to the detectors. Figure 3 shows modeled photocurrent in the detector as a function of longitudinal separation between fiber and detector. For short separations, the PIN generates a larger photocurrent due to it higher responsivity, but as the separation increases the PIN photocurrent drops off much more quickly than that of the I-MSMs or MSMs due to the smaller surface area of the PIN. Photocurrent as a function of transverse separation is shown in Figure 4. To realize a fair comparison of alignment tolerance of the MSMs and PIN, note that the curve shown for the PIN represents a longitudinal separation of 1 mm, while the curves for the I-MSMs and MSMs represent a longitudinal separation of 5 mm. Comparing both types of detector at one longitudinal separation would be to the detriment of one of the detectors. Figures 5 and 6 show similar curves for the same detectors and fibers but use a Lambertian beam instead of a Gaussian. In Figure 6, the longitudinal separation between fiber and detector is 500 μm and 100 μm for the MSMs and PIN, respectively. For both types of beams, the large detecting areas of the MSMs make them much more alignment tolerant than the PIN, and the large responsivity of the I-MSMs accounts for a higher degree of alignment tolerance than that exhibited by conventional MSMs.

Due to the high attenuation of step-index plastic optical fiber (POF) at far infrared wavelengths, a wavelength of 650 nm was used to model the POF links. Other link parameters, including detector size and responsivity were not modified, but a change in wavelength implies the use of another material such as GaAs for detector fabrication since InGaAs does not efficiently absorb photons at the shorter wavelength. The results of the POF link modeling are presented in Figures 7 – 10. Figure 7 shows modeled photocurrent in the detector

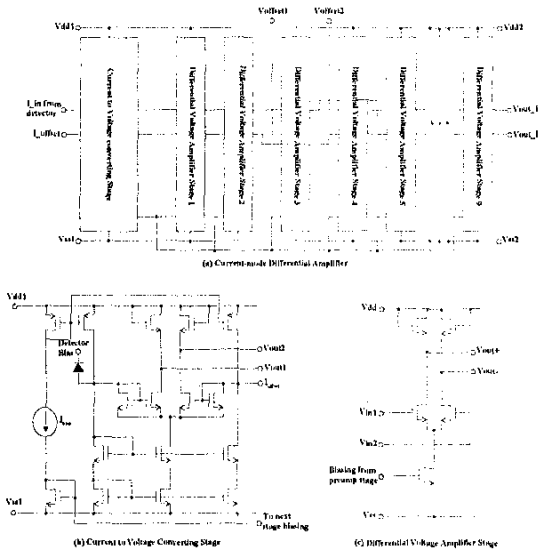

Figure 11: Circuit diagram of the fully differential current input receiver circuit

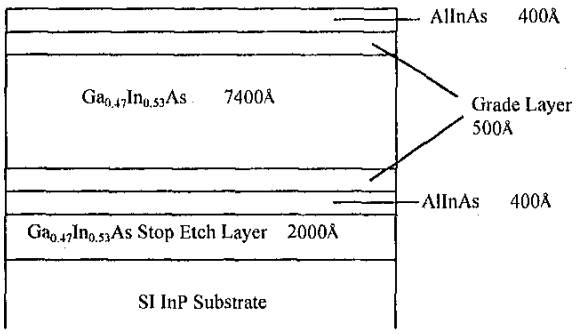

Figure 12: I-MSM structure – all layers nominally undoped

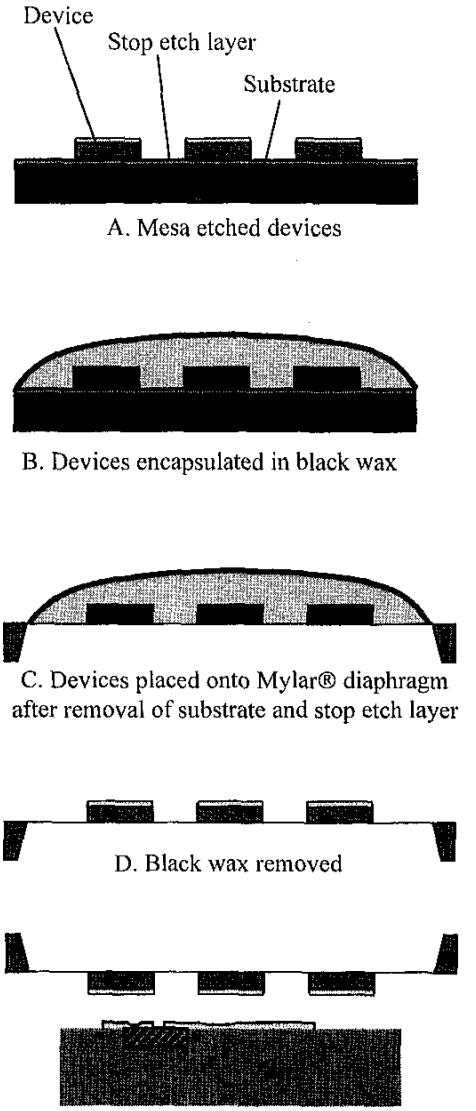

Figure 13: Device fabrication and integration

as a function of longitudinal separation between fiber and detector for Gaussian beam input, and Figure 8 shows the photocurrent as a function of transverse separation. The large areas of the MSMs and I-MSMs enable considerable degrees of longitudinal alignment tolerance with little decrease in photocurrent exhibited for longitudinal separations as large as 10mm. Although PIN photocurrent does not decrease much with longitudinal separation, the small size of the detector compared to the beam width and fiber core diameter prevents the majority of beam power from coupling to the detector. For this reason, the PIN photocurrent is significantly less than that of the MSMs and I-MSMs. In fact, the PIN photocurrent is less than the necessary 2.3 μA required for receiver operation. The MSMs and I-MSMs are highly alignment tolerant for transverse separations as well.

Figures 9 and 10 show similar comparisons of MSM, I-MSM and PIN alignment tolerance for the case of POF Lambertian beam input. The MSMs and I-MSMs exhibit high degrees of alignment tolerance for both longitudinal and transverse separations. As in the POF Gaussian beam input case, the small size of the PIN compared to fiber core diameter results in photocurrents less than 2.3μA. For all three types of photodetectors, Gaussian beams provide a greater degree of longitudinal alignment tolerance in the receiver link due to the highly directional nature of the beam, whereas the links using Lambertian beams exhibit greater degrees of transverse alignment tolerance.

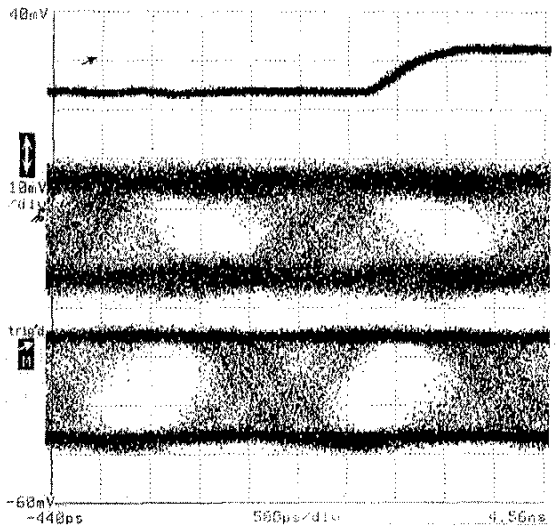

Figure 14: Eye diagram of differential receiver output at 414 Mbps

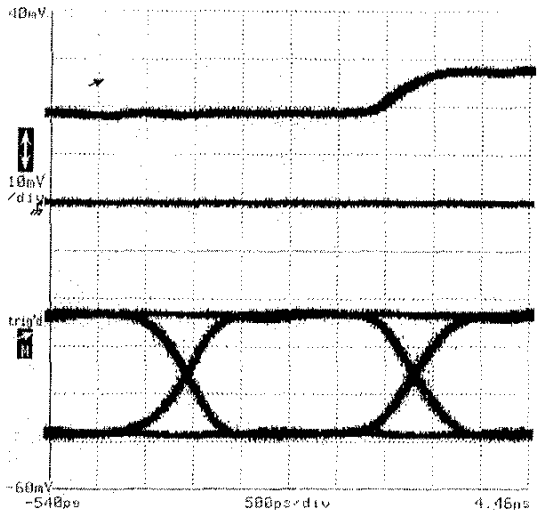

Figure 15: Eye diagram of comparator output at 414 Mbps

Receiver Circuit

Designing sensitive optoelectronic receivers for operation in the presence of digital noise is a challenge and a barrier to the implementation of smart photonic circuitry with digital circuits on an HDI/HDW substrate in a mixed signal environment due to the noise from the digital circuitry. Previous research indicates that the level of this noise can exceed several tens of millivolts and this level is sufficient to impair the operation of analog OE interface circuitry.

The differential receiver designed, tested, and integrated for this work has a fully differential current mode input, current to voltage conversion, and voltage gain stages, as shown in the circuit design in Figure 11.

Fabrication of the Hybrid Optoelectronic Receiver Interface

The hybrid optoelectronic receiver shown in Figure 1 utilizes an I-MSM that was independently grown and optimized, and was subsequently bonded directly to the Si CMOS differential receiver circuit. This hybrid integration approach enables independent circuit and OE device optimization, and can also reduce packaging parasitics that are typically associated with hybrid packaged receivers (i.e., the OE device and receiver are packaged separately). One example of this reduction in packaging parasitics in the elimination of the use of 50 ohm impedance lines between the OE device and the circuit in a hybrid package. The receiver performance can be improved through hybrid integration of the detector onto the receiver circuit because it enables the use of a high impedance input to the receiver, resulting in a lower

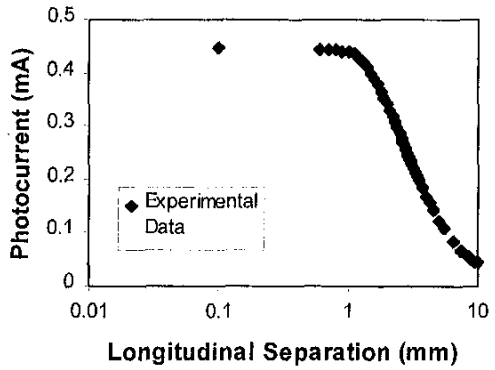

Figure 16: Measured photocurrent in the I-MSM as a function of longitudinal separation

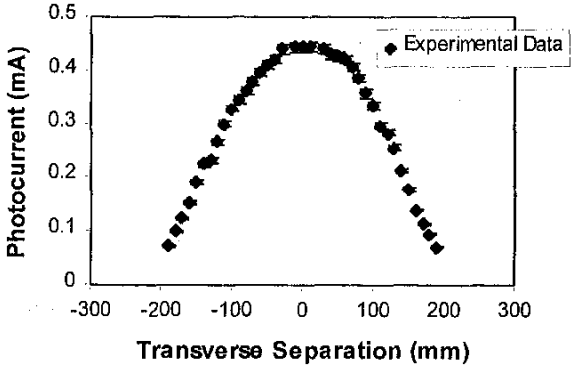

Figure 17: Measured photocurrent in the I-MSM as a function of transverse separation at 1 mm of longitudinal separation

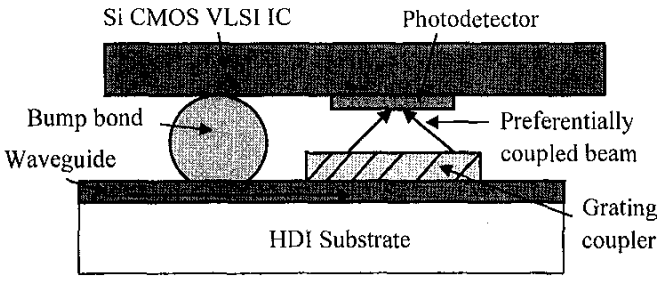

Figure 18: Integration scheme for OE interface to HDI substrate

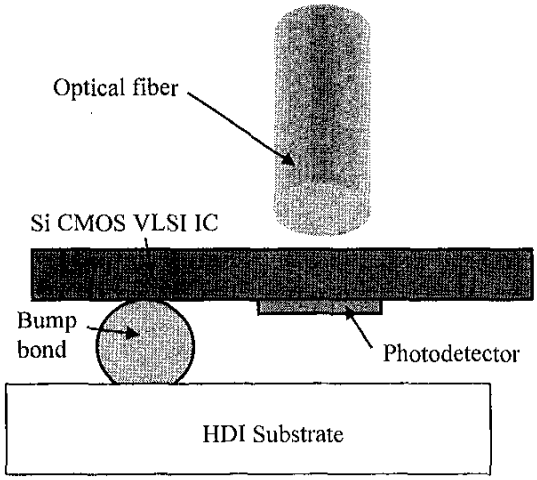

Figure 19: Integration scheme for OE interface to HDI substrate

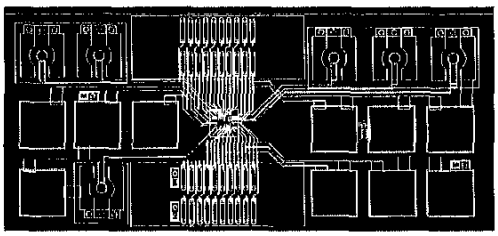

Figure 20: Layout of SLIM substrate

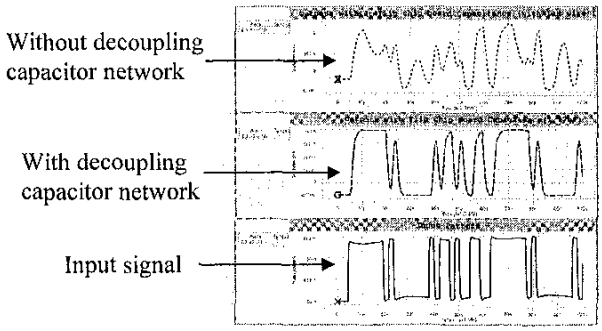

Figure 21: SLIM HDI/HDW substrate simulation results

noise receiver.

Figure 12 shows the layer structure of the I-MSM used in the receiver. The layers were grown on an InP substrate by molecular beam epitaxy (MBE). Ti/Au electrodes and contact pads were deposited and defined photolithorgraphically on the semiconductor surface. Mesas were then photolithographically defined, and device mesas were wet-etched down to the InGaAs stop etch layer. The devices were encased in a protective layer of black wax, and the substrate and stop etch layer were removed. The exposed undersides of the devices were then bonded to a Mylar® transfer diaphragm, and the black wax was removed. The devices may then be selectively bonded onto circuits, test pads, or any other relatively smooth host substrate. Figure 13 summarizes the substrate removal and device integration steps. After the detector is integrated onto the circuit, polyimide (PI 2611) is spun onto the cirucit and cured for two hours at 200°C. The polyimide is then removed via an RIE etch. This final step of polyimide cure and removal improves the reliability of the metal-metal bond.

Integrated Receiver Test Results and Alignment Tolerance Measurements

To test the integrated receiver shown in Figure 1, a Fabry-Perot laser operating at 1.3 μm was used as the optical source. The laser was pigtailed to a glass single mode optical fiber that was then coupled to a glass graded-index (GRIN) multimode fiber with a core diameter of 62.5 μm and a numerical aperture of 0.275. The output end of the multimode fiber was cleaved and positioned above the integrated receiver using a fiber chuck and an XYZ translation stage. The laser was driven by a bit error rate (BER) transmitter, and the outputs of the differential receiver were fed directly into the comparator in the BER receiver.

The fiber was aligned to the detector in the longitudinal direction by sight, so the initial longitudinal separation between fiber and detector is uncertain but is assumed to be approximately 100 μm. To determine the location of the center of the detector to measure alignment tolerance, the fiber was moved in both the +x and -x direction over the the fiber until the 3 dB decrease in photocurrent was reached in each direction. The center of the detector along the x-axis was then taken to be the midpoint between the two –3 dB points. The same procedure was performed for the y-axis in order to locate the center of the I-MSM.

The receiver operated a data rate of 480 Mbps with a BER of 0.1×10^{-10}. At 414 Mbps, the BER was 10^{-11}. Figure 14 shows the eye diagram of the differential receiver outputs at 414 Mbps, and Figure 15 shows the eye diagram of the comparator output at the same data rate.

Alignment tolerance measurements were performed at 200 Mbps. Figures 16 and 17 show the experimental results of the

measurements. The transverse alignment tolerance measurements shown in Figure 17 were taken with a longitudinal separation of 1mm. These results demonstrate that the use of the I-MSM results in a high degree of alignment tolerance for the receiver. The 3 dB decrease in photocurrent occurs either when the fiber and detector are longitudinally separated by 3 mm or when they are misaligned in the transverse direction by ±130 μm.

Alignment Tolerant OE for High-Density Wiring Substrates

The hybrid integrated receiver circuit OEICs used in this research were designed for bump bonding to HDI/HDW substrates for high bandwidth optical signal distribution. Due to the thin film nature of the photodetector, these hybrid OEIC receiver interfaces can be bump bonded to a substrate (conventional photodetectors with the substrate attached would preclude bumping due to the height of the detector). There are a number of schemes through which the interface can be optically addressed, including through integrated waveguides on the substrate with grating coupling, or through back-illumination using an external optical fiber (in this case, the MSM should be integrated with the fingers on the top of the device for back illumination). The back-illuminated OE interface to an HDW substrate requires operation at a wavelength of either 1.3 or 1.55 μm so that the Si CMOS will be transparent to the incident signal. Figures 18 and 19 illustrate the two integration schemes described above. Figure 20 shows the layout for the single level integrated module (SLIM) HDI substrate for which the integrated recevier OEIC was designed. This substrate is currently in process.

The SLIM substrate shown in Figure 20 has embedded passive capacitors which form a decoupling network. Decoupling networks are used to prevent supply voltage fluctuations in the presence of high frequency supply current variations, and to prevent high frequency signal feedback to potentially sensitive bias inputs. The decoupling capacitors embedded in the HDI/HDW SLIM substrate have been designed for a value of 1.77 nF. Figure 21 shows the simulation of the SLIM HDI/HDW substrate with and without the embedded decoupling capacitor network. The signal integrity is highly improved with the inclusion of the decoupling network in the substrate.

Conclusions

High frequency signal distribution in HDI/HDW substrates can be achieved using optical interconnections. To realize effective milli- and micro-haul interconnections on these substrates, the hybrid integration of independently optimized interface circuits and optoelectronic detectors is critical. Further, to realize effective cost goals, designing the optoelectronic interface for alignment tolerance is a key goal. Realization of these interfaces bump bonded to HDI/HDW substrates will enable high speed, low latency optical interconnections for milli- and micro-haul interconnections.

Acknowledgments

The authors would like to thank the National Science Foundation for support of this work through the Packaging Research Center, the Packaging Research Center and Microelectronics Research Center Staff for their research and fabrication assistance.

References

1. Vendier, O., Jokerst, N., Leavitt, R., "Thin-Film Inverted MSM Photodetectors," *IEEE Photonics Technology Letters*, vol. 8, no.2 (February 1996), pp.266-8.
2. Wang, S., Ingram, M., "A novel Fourier technique for calculating fiber-to-LED coupling efficiency with lateral and longitudinal misalignments," *Journal of Lightwave Technology*, vol. 14, no. 10 (Oct. 1996), pp. 2407-13.
3. Hsu, S., King, O., Johnson, F., Hryniewicz, J., Chen, Y., Stone, D., "InGaAs pin detector array integrated with AlGaAs/GaAs grating demultiplexer by total internal reflector," *Electronics Letters*, vol. 35, no. 15 (22 July 1999), pp. 1248-9.